MIPAS MICROWINDOWS

Anu Dudhia[1] **and Victoria Jay**[2]

[1]*Atmospheric, Oceanic & Planetary Physics, University of Oxford, Parks Rd, Oxford OX1 3PU, UK*
Email: dudhia@atm.ox.ac.uk
[2]*Rutherford Appleton Laboratory, Chilton, Didcot, OX11 0QX, UK, Email: V.L.Jay@rl.ac.uk*

ABSTRACT

Spectrally resolving infrared instruments such as the Michelson Interferometer for Passive Atmospheric Sounding generate measurements at a far greater rate than can be accurately modelled within a retrieval. For limb-viewing instruments the usual approach is to select microwindows: subsets of the spectrum of a few cm^{-1} width which maximise the information on the target species while minimising the contributions from potential error sources such as emissions from other molecules. Here, the algorithm used to select microwindows for ESA's Level 2 processing of MIPAS data is outlined, together with some examples of its application.

Key words: MIPAS, microwindows, retrieval, error analysis.

1. INTRODUCTION

The Michelson Interferometer for Passive Atmospheric Sounding (MIPAS) was launched on ESA's Envisat satellite on 1st March 2002. MIPAS is a Fourier transform spectrometer with a maximum optical path difference of 20 cm, giving spectra sampled at 0.025 cm^{-1} (actual resolution is closer to 0.035 cm^{-1}), split into 5 bands in the range 685–2410 cm^{-1}, or 14.5–4.1 μm (Fig. 1).

MIPAS scans the atmospheric limb with a field-of-view approximately 3 km high × 30 km wide. Usually viewing is in the rearward direction although it also has the capability to view at 90° to the orbital track. In the nominal observing mode, a spectrum is acquired every 4.6 seconds at each of 17 tangent altitudes starting at 68 km and finishing at 6 km (3 km steps between 42–6 km). A complete limb scan is obtained approximately every 80 seconds, or 500 km along-track (Fig. 2), giving over 1000 profiles a day.

MIPAS operated in nominal mode from July 2002 until March 2004 when it was switched off following increasingly frequent problems with the interferometer slide mechanism. The instrument was reactivated in August 2004 using a slide movement reduced by a factor 2.5, hence a wider spectral sampling of 0.0625 cm^{-1}.

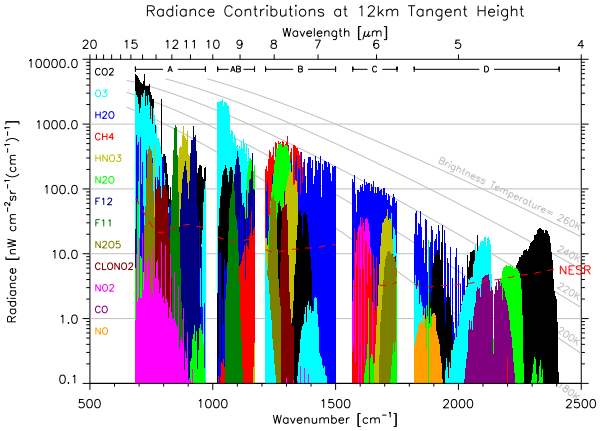

Figure 1. The regions of the infrared spectrum covered by the 5 bands of MIPAS, showing the emission features of some of the most significant molecules, calculated for a limb view of tangent height 12km (approx. 200 mb). The red dashed line represents a typical value of the Noise Equivalent Signal Radiance (NESR).

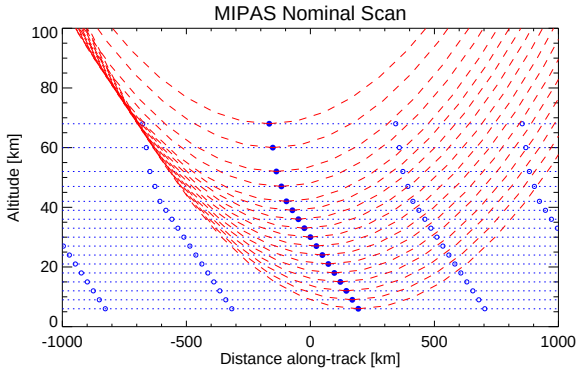

Figure 2. The tangent paths (dashed red lines) and tangent points (solid blue circles) for a nominal MIPAS rear-viewing limb scan, with the satellite to the right and moving right. Open circles show tangent points from successive scans.

2. THE INFRARED SPECTRUM

Fig. 1 shows the infrared spectrum observed by MIPAS for a tangent height of 12 km. At the resolution of this plot (1 cm^{-1}) the spectral features of the different molecules are too dense to be separated, allowing signatures from only a few of the major species to be distinguished unambiguously. However, expanding the spectral axis (Figs. 3 and 4) to the MIPAS resolution it can be seen that there are clear gaps between the lines which can be exploited to detect minor species.

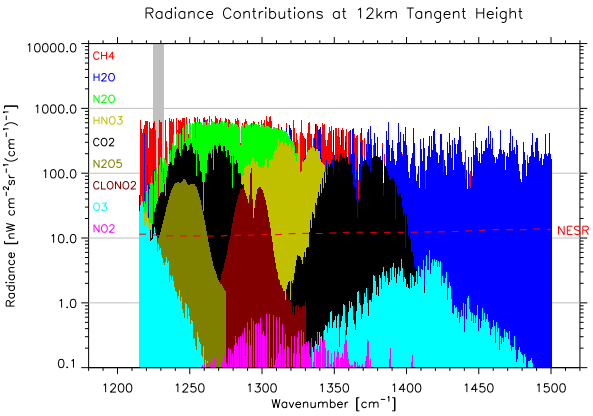

Figure 3. Expansion of Fig. 1 showing the MIPAS band B in detail. The shaded region is shown further expanded in Fig. 4.

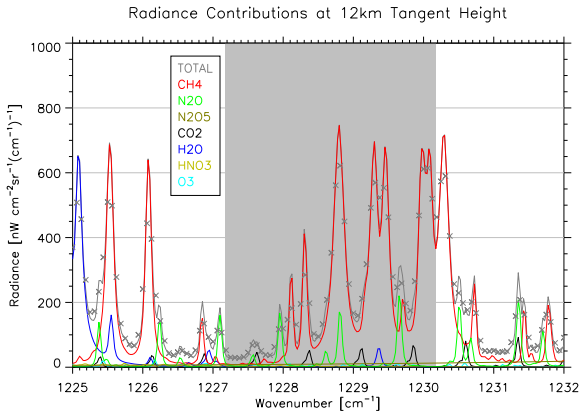

Figure 4. Expansion of Fig. 3, and changing to a linear radiance scale, showing the 1225–1232 cm^{-1} region in detail at MIPAS' original 0.025 cm^{-1} resolution. The grey curve, mostly obscured by the CH_4 contribution, shows the total radiance spectrum and the crosses the equivalent spectrum at 0.0625 cm^{-1} resolution. The shaded region shows the spectral position of the primary CH_4 microwindow used in the operational retrieval.

Fig. 4 shows that MIPAS can distinguish individual spectral lines, but the underlying atmospheric spectrum (Fig. 5) has significantly more structure. The MIPAS spectra reproduce the pressure-broadened features characteristic of upper tropospheric emissions but not the Doppler-broadened 'cores' emanating from the upper stratosphere. Although such sharp features cannot be resolved, nevertheless they do contribute significantly to the total radiance. Therefore the spectral grid for the radiative transfer calculation within the retrieval forward model has to be sufficiently fine (typically 0.0005 cm^{-1}) to capture this structure.

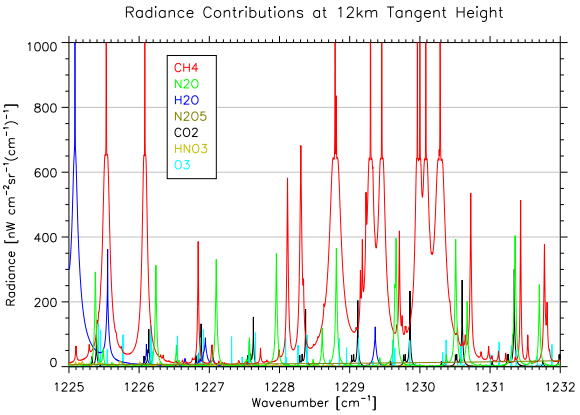

Figure 5. The same spectral region as Fig. 4 but showing the atmospheric radiance spectrum reaching MIPAS, prior to convolution with the instrument line shape.

3. MICROWINDOWS

The measurement domain for a spectrally resolving limb sounder can be considered to be a two-dimensional grid of tangent altitude versus spectral channel. In principle it is possible to use individual measurements within this domain, or individual spectral channels over a range of tangent heights[1], but for limb sounding it is more common to use 'microwindows': rectangular subsets of the measurement domain of widths up to a few cm^{-1}.

The main physical reason for using microwindows is to allow a spectrally flat atmospheric continuum profile to be retrieved within each region, so that the retrieval of the target molecule is based on the amplitude of the line structure relative to the background emission rather than its absolute magnitude. This makes the retrieval insensitive to the presence of spectrally-smooth features such as aerosols, thin clouds or poorly-modelled line wing contributions (e.g., the H_2O continuum). However, the disadvantage of a joint continuum retrieval is the reduced retrieval sensitivity to the heavier molecules (N_2O_5 being a notable example) which tend not to have a resolvable spectral line structure.

A second advantage is numerical efficiency. Forward models (for MIPAS-type instruments) are usually based on monochromatic, pencil-beam calculations which are

[1]The single channel approach is, in fact, commonly used with nadir sounding spectrometers. However, there is insufficient information in the nadir view to fit a continuum profile and the forward models are often highly parameterised (to cope with the faster acquisition rates) so that the benefits of the microwindows approach are less evident.

then convolved with the instrument line shape (ILS) (spectral domain) and field of view (tangent height domain). These are more efficient if microwindows are used and the forward calculation is itself more efficient if multiple tangent heights are used for the same spectral region since the absorption coefficients for many of the path segments (see Fig. 2) can be reused within a single profile retrieval.

Fig. 6 shows the locations of the microwindows used for ESA's 'off-line' retrievals[2], together with a plot of the spectral features of the target molecules. Since each species is retrieved separately the microwindows are positioned to select spectral regions where the lines of the target molecule dominate, CO_2 lines being used for the pressure-temperature (pT) retrieval. For pT, O_3 and H_2O, the tangent altitude range of the microwindows varies according to the strength of the spectral absorption feature, i.e., using the strongest absorption regions for high altitudes and weaker features for low altitudes.

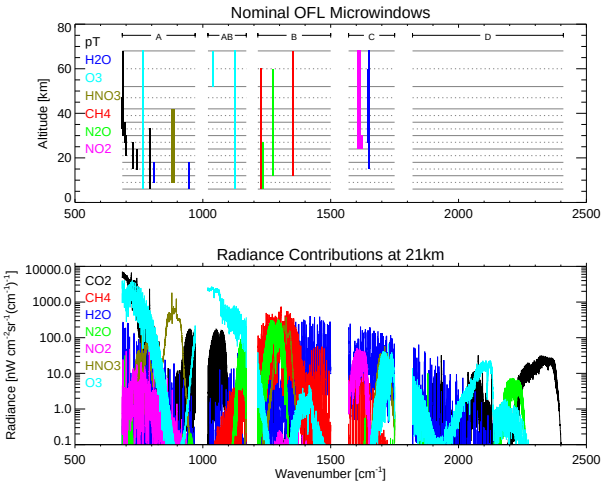

Figure 6. The upper plot shows the spectral locations and tangent altitude range of the microwindows used for the MIPAS 'off-line' retrievals (note that the actual spectral width of each microwindow — maximum 3 cm^{-1} — is too narrow to be shown to scale on these plots). The lower plot shows the emission features of the target molecules in the MIPAS spectrum calculated for 21 km tangent altitude. No operational microwindows are selected in band D (mainly due to poor signal/noise).

It should be noted that only a few percent of the measurements in the complete spectra are actually used in the retrieval. The high CPU cost of running the forward model limits the number of measurements that can be used so the aim is to determine the microwindows which give the greatest retrieval accuracy for the minimum computation effort[3].

[2]Mostly these are the same microwindows as used for the 'near-real-time' retrievals, the main difference being the reduced tangent altitude range used in the near-real-time processing

[3]In nadir sounding, highly parameterised forward models or statistical techniques such as principal component analysis are often used in order to process data at the generally higher data rates (typically measured in profiles/second rather than profiles/minute). However, for a research instrument such as MIPAS the preference has been for the accuracy and robustness offered by a using a physical forward model.

In the past these microwindows have been 'hand-selected', but for the MIPAS operational retrievals a computer algorithm has been developed [1]. This is based on modelling the propagation of a large number of potential sources of error, systematic as well as random noise, through the retrieval process for a variety of atmospheric conditions in order to maximise the accuracy of the retrieved products[4].

4. RETRIEVAL MODEL

The ESA retrieval algorithm [2] is non-linear least squares fit, which, in linearised form, may be represented as the minimisation of the cost function:

$$\chi^2 = (\mathbf{y} - \mathbf{K}\mathbf{x})^T \mathbf{S}_y^{-1} (\mathbf{y} - \mathbf{K}\mathbf{x}) \quad (1)$$

where $\mathbf{y}$ is the set of measurements with noise covariance $\mathbf{S}_y$, $\mathbf{x}$ is the state vector (i.e., profile to be retrieved) and $\mathbf{K}$ the *Jacobian* (or *Weighting Function*) matrix with elements $K_{ij} = \partial y_i / \partial x_j$.

This has the standard solution (e.g., [3])

$$\mathbf{x} = \mathbf{G}\mathbf{y} \quad (2)$$

where $\mathbf{G}$ is the *Gain* (or *Contribution Function*) matrix with elements $G_{ji} = \partial x_j / \partial y_i$ given by

$$\mathbf{G} = \left(\mathbf{K}^T \mathbf{S}_y^{-1} \mathbf{K}\right)^{-1} \mathbf{K}^T \mathbf{S}_y^{-1} \quad (3)$$

Therefore it follows that the solution covariance $\mathbf{S}_x$ is related to the measurement covariance $\mathbf{S}_y$ by

$$\mathbf{S}_x = \mathbf{G}\mathbf{S}_y\mathbf{G}^T \quad (4)$$

$$= \left(\mathbf{K}^T \mathbf{S}_y^{-1} \mathbf{K}\right)^{-1} \quad (5)$$

5. TOTAL ERROR

The retrieval (Eq. 2) assumes a Gain matrix $\mathbf{G}$ based only on the random noise component of measurement error $\mathbf{S}_y \equiv \mathbf{S}_y^{\mathrm{rnd}}$. Noise in the raw spectra is assumed uncorrelated, but correlations introduced by the smoothing effect of the apodisation are accounted for as off-diagonal elements of $\mathbf{S}_y^{\mathrm{rnd}}$.

However, there are a number of additional sources of error in measurements or in the forward model (Table 1, and discussed further in section 10) which, although not included in the retrieval itself, can be modelled retrospectively. Representing each of these errors i as an independent error covariance matrix in the measurement domain $\mathbf{S}_y^i$, the *total measurement error* covariance is then given by:

$$\mathbf{S}_y^{\mathrm{tot}} = \mathbf{S}_y^{\mathrm{rnd}} + \sum_i \mathbf{S}_y^i \quad (6)$$

[4]ESA's data processing can use different sets of microwindows optimised for particular latitude bands and seasons, but in practice just one set of microwindows is applied globally. This is less optimal in terms of accuracy, but avoids retrieval artefacts associated with changes between microwindow sets.

Table 1. MIPAS error sources, in addition to random noise, and estimates of 1 σ uncertainty ('Code' refers to symbols in Figs. 13 and 14).

Error Source	$1\,\sigma$	Code
Errors in Instrument Characterisation		
Radiometric Gain	$\pm 2\%$	GAIN
Spectral Calibration	$\pm 0.001\text{cm}^{-1}$	SHIFT
Apodised ILS Width	$\pm 2\%$	SPREAD
Errors in Forward Model Parameters		
Profiles of 28 gases	Climat.SD[1]	[gas]
High Alt. Column	Climat.SD[1]	HIALT
Line database errors	(See Note[2])	SPECDB
Continuum model	$\pm 25\%$	CTMERR
Retrieved p error	$\pm 2\%$[3]	PRE
Retrieved T error	± 1 K[3]	TEM
Deficiencies in Forward Model		
Non-LTE effects	Modelled	NONLTE
CO_2 Line Mixing	Modelled	CO2MIX
Horiz.T gradients	$\pm$1K/100km	GRA

Notes
[1] Uncertainty with which climatology represents the actual local state of the atmosphere
[2] Based on assumed accuracies in line parameters
[3] Impact of pT retrieval errors on subsequent constituent retrievals

where Following the form of Eq. 4, this gives a *total retrieval error* covariance:

$$\mathbf{S}_x^{\text{tot}} = \mathbf{G}\mathbf{S}_y^{\text{rnd}}\mathbf{G}^T + \mathbf{G}\left(\sum_i \mathbf{S}_y^i\right)\mathbf{G}^T \quad (7)$$

$$= \mathbf{S}_x^{\text{rnd}} + \sum_i \mathbf{S}_x^i \quad (8)$$

$$= \mathbf{S}_x^{\text{rnd}} + \mathbf{S}_x^{\text{sys}} \quad (9)$$

Note that the definition of $\mathbf{G}$ itself (Eq. 3, with $\mathbf{S}_y \equiv \mathbf{S}_y^{\text{rnd}}$) is unchanged since this is fixed by the retrieval algorithm. Eq. 8 forms the basis of the error analysis, discussed in section 10.

6. INFORMATION CONTENT

Having established a formulation of the *total error*, or 'accuracy', profile of the retrieval for a given set of measurements, the next step is to express this as a single scalar quantity, or 'Figure of Merit', which allows the retrievals from different sets of measurements to be directly compared. One possible such parameter is the the *(Shannon) Information Content* (e.g., [3]), H, defined as:

$$H = -\frac{1}{2}\log_2\left|\mathbf{S}_x\mathbf{S}_a^{-1}\right| \quad (10)$$

where $\mathbf{S}_x$ is the retrieval (or *a posteriori*) covariance, $\mathbf{S}_a$ is the *a priori* covariance and $|\ldots|$ indicates the determinant. H is measured in bits. In simple terms, if the retrieval reduces the variance at one profile level by a factor 4 (i.e., a factor 2 in standard deviation) this corresponds to 1 bit of information.

There is no explicit *a priori* estimate in the ESA retrieval but the information can be defined in terms of an improvement over a 'climatological' covariance $\mathbf{S}_a$, e.g., for volume mixing ratio retrievals a diagonal matrix with elements corresponding to 100% uncertainty in concentration[5]. However, this means that the absolute value of the information content of the MIPAS retrieval is somewhat arbitrary.

There is the issue as to whether the retrieval covariance $\mathbf{S}_x$ in Eq. 10 should represent just the random error covariance $\mathbf{S}_x^{\text{rnd}}$ or total error covariance $\mathbf{S}_x^{\text{tot}}$ from Eq. 9 (it is assumed that the *a priori* covariance $\mathbf{S}_a$ is purely random). The former would correspond to maximising retrieval *precision* (i.e., selecting measurements with maximum signal/noise) while the latter, as actually used for MIPAS microwindows, maximises retrieval *accuracy*.

For the selection of the microwindows for operational processing, the 'Figure of Merit' also incorporates an estimate of the CPU cost of each microwindow as well as its information content.

7. GROWING MICROWINDOWS

The scheme described shows how microwindows can be compared but not how the microwindows themselves are determined.

The procedure is to evaluate the information content of every individual point within the measurement domain. Those with the highest information are then used as 'seeds' about which trial microwindows are grown, as illustrated in Fig. 7. This method allows for measurements within the microwindow to be excluded ('masked') if their net contribution to the retrieval information content is negative[6]. Fig. 8 shows the spectral masks associated with the primary CH_4 microwindow.

The best microwindow is incorporated in the retrieval model, the resulting retrieval covariance then replaces climatology as the *a priori* covariance in the definition of information content (Eq. 10), and the process is repeated with the remaining individual measurements being re-evaluated with this new definition of information. This continues until either the required maximum number of microwindows is found or no further microwindows can be found which increase the information of the retrieval.

[5] For the pT retrieval the ESA processing does use *a priori* information in the form of the knowledge of the relative separation of the tangent heights from the instrument pointing, which is coupled to the pT retrieval via the hydrostatic constraint. In the selection of pT microwindows this is represented by a highly-correlated *a priori* pressure covariance, although the temperature covariance has only diagonal elements of $(10\text{ K})^2$.

[6] The concept of 'negative information' arises because the retrieval weights measurements considering only the random noise component of error, whereas the definition of information content allows for additional error sources. Basically, incorporating such measurements would result in an increase in systematic error which outweighed their reduction in the random error.

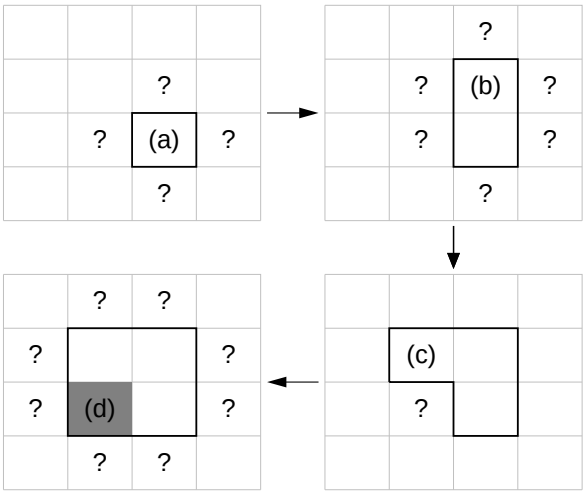

Figure 7. Diagram illustrating the procedure used to 'grow' microwindows in the measurement domain. Starting with a single measurement (a), adjacent points are tested and the microwindow (indicated by thick lines) expanded to incorporate the point (b) which adds the most information. The process is then repeated for the new perimeter. Having added a point (c), in order to keep the microwindow rectangular, remaining points along the same boundary are also incorporated, but may be excluded ('masked') (d) if they contribute negative information. The process continues until either the maximum size is reached (17 tangent altitudes × 3 cm^{-1}) or the addition of any further measurements results in a decrease of information.

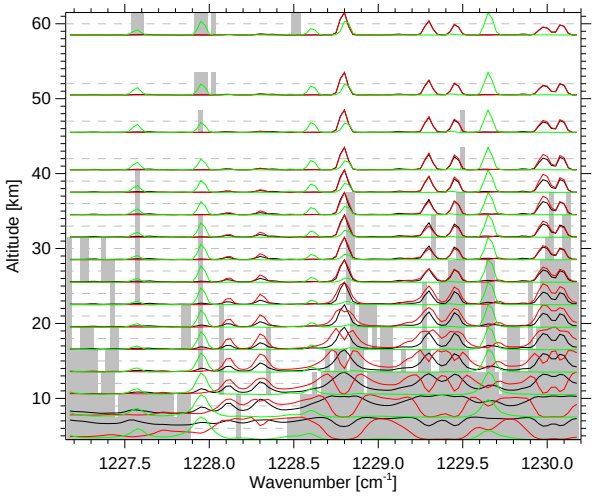

Figure 8. The primary CH_4 microwindow used in the operational MIPAS retrieval. The grey boxes indicate the spectral masks. Superimposed for each tangent altitude are (arbitrarily scaled) curves representing total radiance (black), CH_4 Jacobians (red) and Jacobians of N_2O (green) — a major contaminant gas in this microwindow. Note that the masks often, but not always, correspond to N_2O lines, or regions where the sensitivity to CH_4 is low compared to the total radiance (e.g., the strong line at 1228.8 cm^{-1} which is saturated at low altitudes).

8. ROLE OF THE CONTINUUM RETRIEVAL

The original intention of simultaneously retrieving a continuum profile for each microwindow was described in section 3. However, the accuracy of the continuum retrieval is not incorporated into the definition of information content used by the microwindow selection algorithm. This leads to a further, unanticipated, benefit which is that the continuum retrieval is also used as a sink for systematic errors, including those which do not have any obvious continuum-like structure in the measurement domain.

Most systematic errors would introduce an error of consistent sign into the retrieval, and it would not be expected that such errors would be reduced by adding more microwindows subject to the same systematic error. For example, if the concentration of a contaminant gas is underestimated, its contribution to the total radiance will be underestimated throughout the spectrum and the retrieval will incorrectly increase the concentration, and therefore radiance, of the target molecule to compensate (Fig. 9). However, jointly fitting a continuum within each microwindow provides a mechanism whereby the sign can be reversed, hence the systematic error reduced.

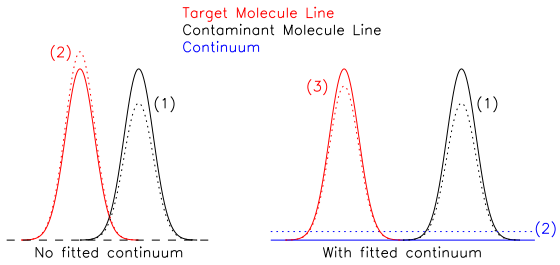

Figure 9. Illustration of the use of the continuum retrieval to invert systematic errors. In the left example, without a fitted continuum, an underestimate of a contaminant concentration (1) will always lead to an overestimate of the target species (2). However, in the right example, where the lines are separated, an underestimate in the contaminant (1) results in an overestimate of the continuum (2), resulting in an underestimate of the target molecule (3).

In order for this compensation mechanism to work, it is necessary that the continuum retrieval is *not* too well constrained by the actual atmospheric continuum and, in order to provide this flexibility, the selection algorithm may insert spectral masks to exclude otherwise valid measurements in continuum regions of the microwindow.

Whatever the precise mechanisms involved, it is at least clear that the control of systematic errors depends on complex interactions between the positioning of spectral masks and the continuum retrieval, which can only really be fully exploited by a computer algorithm. There is the risk that the optimisation will be sensitive to the particular atmospheric conditions and error magnitudes which are modelled, but by simultaneously optimising for a variety of atmospheric conditions some additional robustness can be built into the selection.

9. REDUCED RESOLUTION MODE

To illustrate the microwindow selection procedure, results are presented from a recent investigation into the change in operation to 40% spectral resolution (i.e. from 0.025 cm^{-1} to 0.0625 cm^{-1} sampling). This was performed for all species but only the results for CH_4 are shown.

Microwindows were selected sequentially until, after 6 microwindows, no further microwindows can be found which contribute more than 1 bit of information (as defined in Eq. 10). Fig. 10 shows the location of these microwindows in the measurement domain (which all happened to be in the low-wavenumber end of band B), and note that the first selected microwindow almost coincides with the primary microwindow for the operational retrievals at 0.025 cm^{-1} resolution.

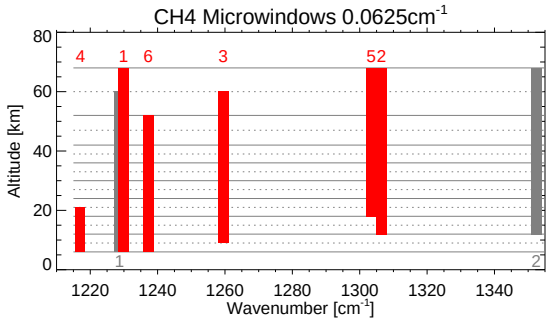

Figure 10. Location of the first six CH_4 microwindows (red) selected for 0.0625 cm^{-1} resolution operation. The numbers indicate the position in the selection sequence. Also shown in grey are the two microwindows used for operational processing at 0.025 cm^{-1} resolution.

Fig. 11 shows the growth in information, defined using either the random or total error covariance, as a function of the number of measurements used (one measurement being a spectral channel at a particular tangent height, so each microwindow can contain up to 49×17=2057 measurements, including masked points).

As mentioned in section 6, the absolute value of information content depends on the choice of *a priori* covariance so the y-axis offset is not particularly significant. The diagonal lines on the plot correspond to the expected slope for the increase of the 'random' information if all microwindows have similar signal/noise characteristics, i.e., a factor 2 reduction in random error SD at all 17 levels (=17 bits) for every factor 4 increase in the number of measurements. This describes the increase in random information content reasonably well, but the total information content falls off as the systematic errors reduce at a slower rate.

Plotted on the same scale are the two microwindows used in the operational retrieval[7]. The number of measurements in this case have been scaled by a factor 0.4

[7]Due to the inclusion of spectral masks, it is not possible simply to re-use the same microwindow at the lower spectral resolution even if the spectral boundaries coincide with the new grid.

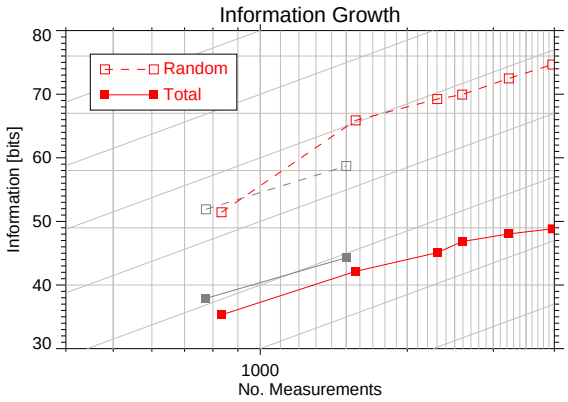

Figure 11. Growth in information as microwindows (represented by the symbols) are added, with information defined either by just the random component of the retrieval error or the total retrieval error. The grey symbols show the two microwindows used in the operational retrievals.

(=0.025/0.0625) in order to represent the total spectral bandwidth (which is a better estimate of CPU cost) of each measurement on the same scale as the 0.0625 cm^{-1} microwindows. It can be seen that, after two microwindows, the total information is slightly less for the lower spectral resolution whereas the random component of information is better.

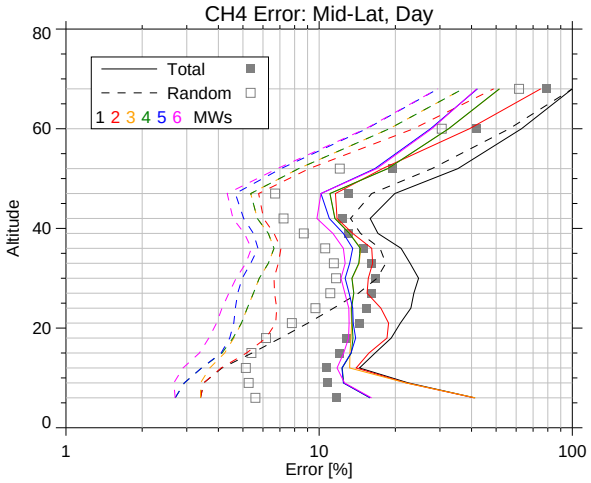

Figure 12. Improvement in the CH_4 retrieval total error (accuracy) and random error (precision) as more microwindows are added. The grey squares show the equivalent profiles for the operational retrieval using two microwindows.

This is illustrated more clearly in Fig. 12, which shows the improvement in accuracy and precision as microwindows are added. Using just two low resolution microwindows gives significantly improved precision than two high resolution microwindows, but although the accuracies are comparable above 27 km, the low resolution microwindows are less accurate at lower altitudes. Even using all 6 low resolution microwindows the accuracy at low altitudes fails to match that obtained with two high resolution microwindows, although the precision continues to improve.

10. ERROR ANALYSIS

The microwindow selection aims to maximise the accuracy of the retrieval by modelling the propagation of not only the instrument noise (as in the operational retrieval) but also other errors in both the measurements and forward model. Therefore, Eq. 8 contains all the information required for a full error analysis of the retrieval. The square roots of the diagonals of each matrix on the right hand side of Eq. 8 correspond to the component of retrieval uncertainty due to each error source. Figs. 13 and 14 shows examples for CH_4 for the operational product and the reduced resolution mode. Note the increased sensitivity to interference from other molecules at the lower resolution.

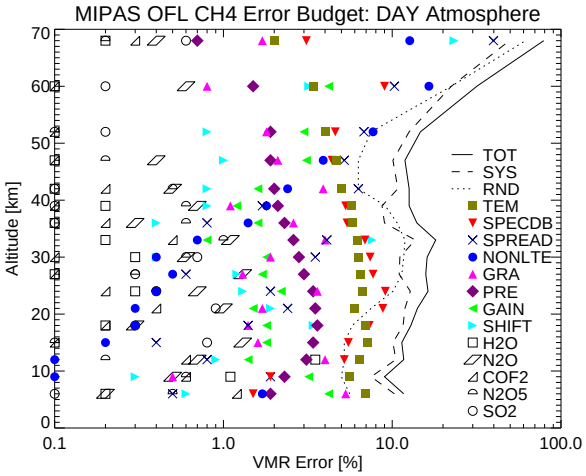

Figure 13. Error analysis for the off-line Level 2 CH_4 product for mid-latitude day-time conditions. The solid line represents the total error, divided into random (dotted) and systematic (dashed) contributions. The various symbols represent the different components of the systematic error (see Table 1), in approximate order of importance.

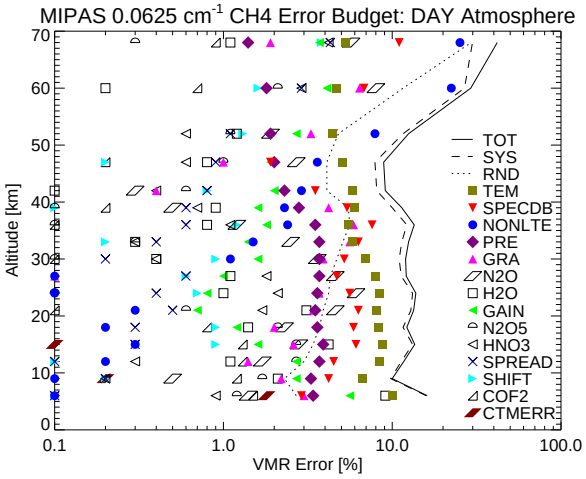

Figure 14. As Fig. 13 but for the reduced resolution ($0.0625\,cm^{-1}$) mode assuming that all six CH_4 microwindows are used.

The term 'systematic error' is used here to describe all errors apart from the noise. Each of these error sources is assumed to introduce some component of correlated error into the measurement (or forward model calculation). In most cases a single error source is considered correlated for *all* measurements, however the following errors are assumed to have localised correlations:

- The radiometric gain (GAIN), ILS width (SPREAD) and spectroscopic database (SPECDB) errors are assumed to be slowly varying in the spectral domain. These errors are modelled as correlated for all measurements within a microwindow (for all tangent altitudes) but uncorrelated between microwindows.
- The pT retrieval errors (PRE,TEM) are assumed to be random, which means that in the constituent retrievals these errors will be correlated for all measurements within the spectrum from a particular tangent height but uncorrelated between spectra from different tangent heights[8].

In these cases, there is effectively a separate error source (or covariance matrix $\mathbf{S}_y^i$ in Eq. 6) for each microwindow or tangent height, but the root-sum-square of these is actually plotted in the figure as a single error.

The systematic error correlations are only defined for the set of measurements that contribute to a single profile, and some care needs to be taken if these error analyses are applied to larger datasets. For example, the spectroscopic database errors would be common to all profiles generated throughout the mission (effectively appearing as a bias term) whereas the pT propagation errors might be random from one profile to the next and disappear with averaging. Other errors would have intermediate timescales depending on atmospheric variability or calibration frequency.

11. OTHER APPLICATIONS

Apart from selecting microwindows for the retrieval of the standard ESA products, the MIPAS microwindow selection program has been applied to a number of other cases.

1. Selection of microwindows for additional species in order to estimate which retrievals are viable and the altitude ranges and accuracies that can be expected
2. Selection of microwindows for MIPAS 'special modes' of operation in which the vertical spacing of the tangent points/retrieval is changed (usually reduced to less than 3 km, thus reducing the relative signal/noise) and/or the spectral resolution is changed (to $0.1\ cm^{-1}$).

[8]The pT errors shown here assume 'typical' temperature and pressure uncertainties of 1 K and 2 % respectively with no vertical correlation. The MIPAS L2 products contain a more accurate representation of the propagation of the pT retrieval errors.

3. Isotopic retrievals. In this case target quantity is the ratio of the minor isotope to the major isotope rather than the absolute concentration of the minor isotope. This leads to a significant cancellation of systematic errors (e.g., sensitivity to temperature retrieval errors) which can be exploited if the microwindows are specifically selected for the ratio retrieval.

4. Joint retrievals. The ESA processing is currently limited to retrieving pT or individual species, which means that pT microwindows, for example, are restricted to regions where emissions are dominated by target species of well-known concentration (i.e., CO_2). However, if pT is retrieved jointly with other species (specifically H_2O and O_3) lines from these molecules can also be used. The microwindows selected for a joint retrieval are therefore generally more efficient (in terms of bits of information per measurement) than separate retrievals.

5. Continuum retrievals. As described in section 8, the microwindow selection for ESA processing treats the continuum retrieval for each microwindow as a sink term for systematic errors. By changing the definition of information content so that the continuum itself is a target species, microwindows can be derived for the retrieval of the background aerosol spectrum and extinction profile.

12. SUMMARY

A microwindow selection algorithm has been developed for MIPAS which attempts to find the spectral regions from which profiles of pressure, temperature and the target molecules can be most efficiently retrieved in terms of maximising the accuracy for a given CPU cost.

This is achieved by modelling not only the random noise contribution but also a number of other, systematic error sources through the retrieval process. A by-product of this selection process is a complete error analysis of the retrieval.

REFERENCES

[1] Dudhia A., Jay V. L. and Rodgers C. D., Microwindow Selection for High-Spectral-Resolution Sounders, *App. Optics*, Vol. 41, 3665–3673, 2002.

[2] Ridolfi M., Carli B., Carlotti M., von Clarmann T., Dinelli B. M., Dudhia A., Flaud J-M., Höpfner M., Morris P. E., Raspollini P., Stiller G. and Wells R. J., Optimized Forward Model and Retrieval Scheme for MIPAS Near-Real-Time Data Processing, *App. Optics*, Vol. 39, 1323–1340, 2000.

[3] Rodgers C. D., *Inverse Methods for Atmospheric Sounding: Theory and Practice*, World Scientific, Singapore, 2000.